

Improving the Rotational Freedom of Polyetherimide: Enhancement of the Dielectric Properties of a Commodity High-Temperature Polymer Using a Structural Defect

Abdullah Alamri,[▽] Chao Wu,[▽] Ankit Mishra, Lihua Chen, Zongze Li, Ajinkya Deshmukh, Jierui Zhou, Omer Yassin, Rampi Ramprasad, Priya Vashishta, Yang Cao,* and Gregory Sotzing*



Cite This: *Chem. Mater.* 2022, 34, 6553–6558



Read Online

ACCESS |



Metrics & More

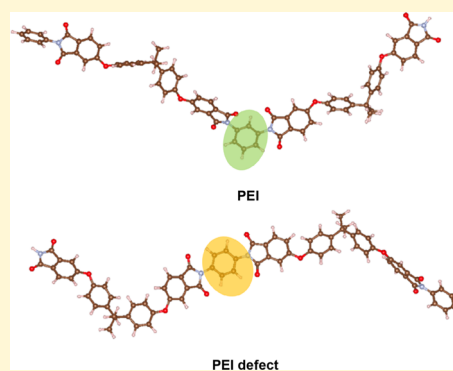


Article Recommendations



Supporting Information

ABSTRACT: Dielectric polymers that can withstand harsh conditions of simultaneous high electric field and elevated temperature are widely used in electrical and electronic systems. However, traditionally, the thermal stability of polymers is engineered based on highly conjugated aromatic molecular structures, giving rise to strong charge transport and thus poor charge–discharge efficiency under concurrent high electric field and elevated temperature. Here, we locally improved the rotational flexibility of the phenylenediamine linkage structure in polyetherimide (PEI) to decouple the conjugation of the organic molecule. *p*-Phenylenediamine (5 mol %) as a low-energy rotation repeat unit within PEI significantly optimized its dielectric properties, exhibiting substantially suppressed electrical conduction (more than 1 order of magnitude lower) and polarization loss (<1%). The new PEI has a largely improved charge–discharge efficiency of 91% at 400 MV/m 200 °C, outperforming the best-reported polymer-based dielectrics without any modification of the cost of goods. The high-throughput facile processing of the new PEI provides a potential candidate for energy storage applications under elevated temperatures. This work unveils a scalable approach to exploring polymer dielectrics by introducing a small amount of local structural modifications.



Capacitive energy storage with high power density is the key to electrification, pulsed power, and electronic systems.^{1–4} The flexibility and scalability of polymer dielectrics coupled with their graceful failure characteristics impart them with irreplaceable advantages compared to ceramic dielectrics.^{3,5} When applied under harsh conditions, electronic systems with large band gap semiconductors and high power density systems all need dielectric materials with superior thermal stability that could withstand elevated temperatures of >150 °C.^{6,7} However, biaxially oriented polypropylene (BOPP), the best commercially available capacitor material, cannot operate continuously when the temperature is above 100 °C.⁸ Established polymers including polyimide (PI), polyetherimide (PEI), and poly(ether ether ketone) (PEEK) with better thermal stability suffered high conduction loss under high electric fields.² Polymers that could function well simultaneously at high electric fields and elevated temperatures are urgently needed for a wide range of applications.

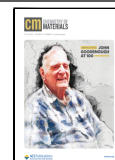
Although inorganic or organic additives with a large band gap could suppress the high field conduction,^{9–12} the unscalable processing of polymer composite films brought huge challenges for industrial manufacturing.^{12,13} To improve the throughput and defect tolerance of inorganic coatings, facile flow-induced self-assembly of two-dimensional (2D) montmorillonite (MMT) nanosheets coating was proposed to

block the charge injection.¹⁴ Although encouraging, further improvements in the electrical properties under extremely high electric fields for the composite dielectrics are still limited by the polymer substrate. A new polymer poly-(oxa)-fluoronorborene (POFNB) was strategically designed through decoupling of the backbone conjugation, exhibiting a large band gap and excellent thermal stability.² A large band gap of polymers led to higher breakdown strength and suppressed electrical conduction. Although polymers have a large design space due to the widely variable chemical space, modifying well-established polymers provides an efficient way for rapid development of polymer dielectrics for industrial applications considering the issues in scaling up. Here, we modified the polyetherimide (PEI), a well-established high-temperature polymer, by introducing small amounts of structural modification to lower the energy for rotation. The improved flexibility is expected to prohibit the localized defect

Received: May 12, 2022

Revised: June 28, 2022

Published: July 12, 2022



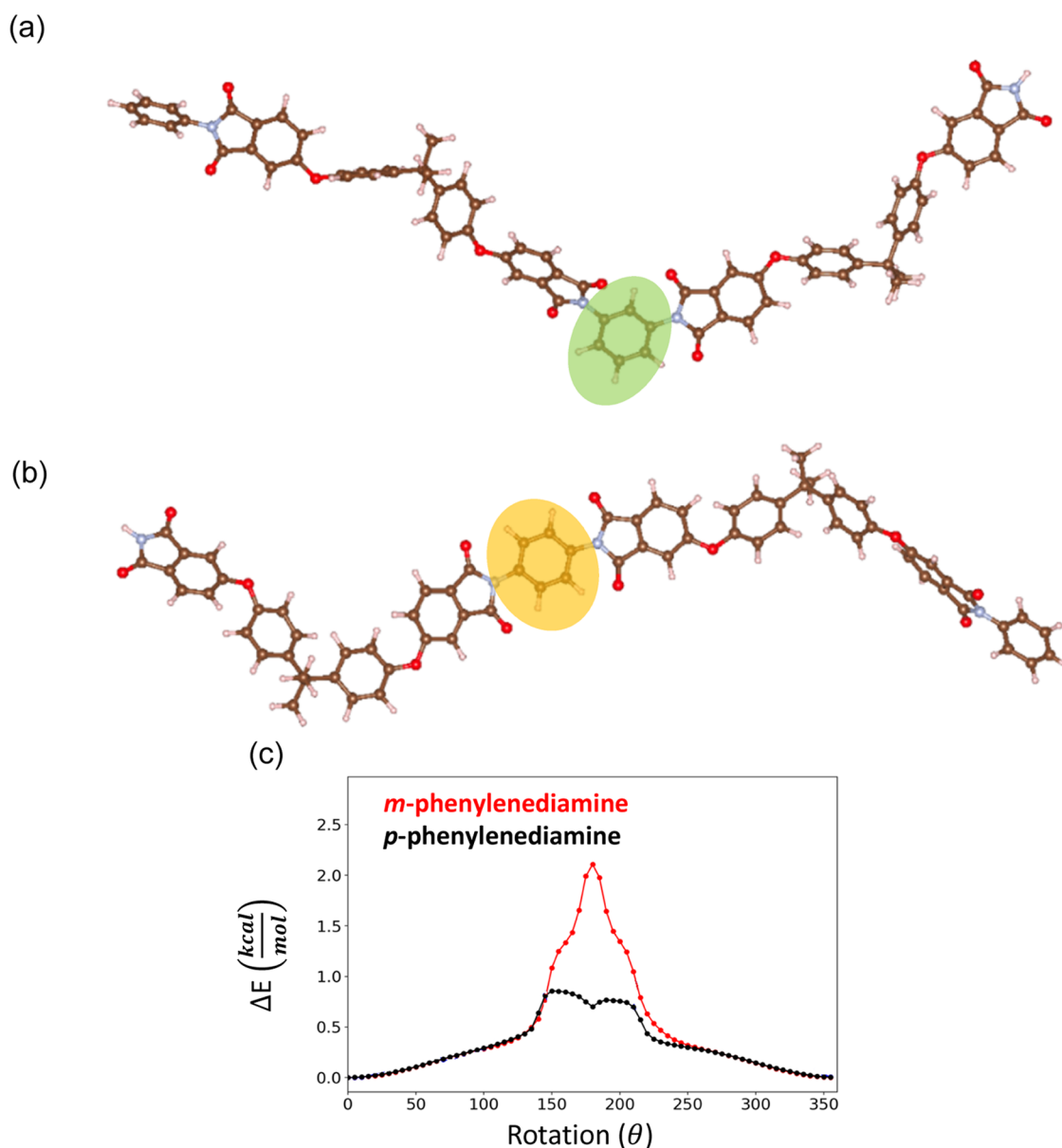


Figure 1. Material design. Schematics of (a) *m*-phenylenediamine and (b) *p*-phenylenediamine in the polymer chain. (c) Rotational energy barrier of the polymer chain.

states, the secondary factor compared to the band gap, by enhancing the interchain interactions. A low polarization loss is also beneficial for improved flexibility.

In this work, PEI with meta phenylenediamine (*m*-phenylenediamine) linkage was synthesized using *m*-phenylenediamine and 4,4'-bisphenol A dianhydride (BisDA). 4-*tert*-Butylaniline was used as the end-capping (Figures S1–S7).¹⁵ Two, five, and ten percent of *para*-phenylenediamine (*p*-phenylenediamine) marked as 2*p*-PEI, 5*p*-PEI, and 10*p*-PEI, respectively, were introduced to modify the polymer structure of PEI. Figure 1a,b highlights the structure of *m*-phenylenediamine and *p*-phenylenediamine linkage in the polymer chain. All polymers are made into films with $\sim 10 \mu\text{m}$ thickness by solution cast for electrical characterizations. To reveal the flexibility of the *p*-phenylenediamine linkage of the modification and the *m*-phenylenediamine linkage in the original PEI, we compute the rotation energy barrier of the N (imide)–C (aromatic) bond using molecular dynamics

simulations, as shown in Figure 1c. The rotation energy barrier around the N (imide)–C (aromatic) bond for the polymer chain with *p*-phenylenediamine linkage is lower than that of the *m*-phenylenediamine linkage, e.g., the maximum rotation energy barrier is decreased from 2.1 to 0.8 kcal/mol. The computation confirmed the design strategy of improving the local flexibility via the introduction of *p*-phenylenediamine as a structural modification. Although the rotation energy barrier of the linkage structure is significantly decreased, the glass transition temperatures of modified PEI and PEI did not show a significant change ($\sim 1\%$). From the DSC spectra in Figure S6, PEI did not show any peaks relevant to the melting process, indicating that PEI did not have any crystalline structures. Therefore, the modification of the polymer structure is considered a local change.

The energy storage properties under a high electric field were investigated using the displacement–electric field loops (DE loops) (Figures S8 and S9). It can be found that 5*p*-PEI

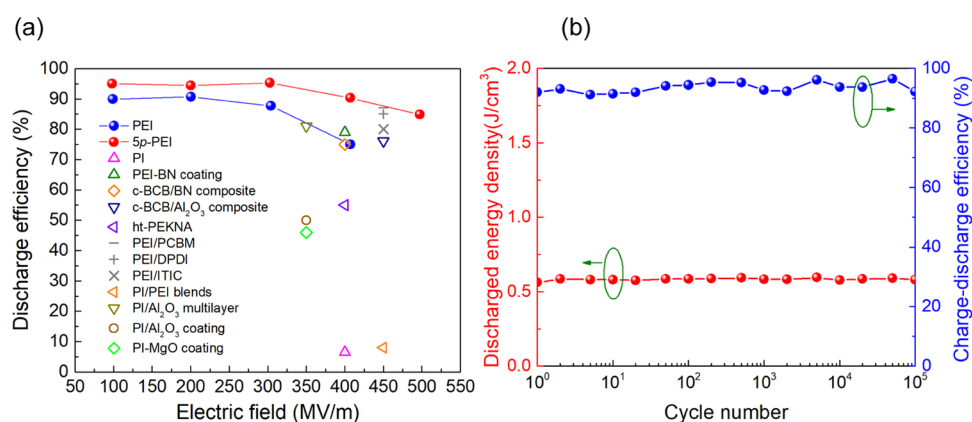


Figure 2. Energy storage performance. (a) Efficiency of PEI in this work in comparison to those of commercial and best-reported polymer-based dielectrics at 200 °C.^{9–12,16–18} (b) Cyclic aging performance of 5p-PEI at 200 °C and 200 MV/m.

exhibits the highest discharge efficiency at room temperature and 150 °C relative to 2p-PEI, 10p-PEI, and original PEI (Figure S10). As 5p-PEI has optimized energy storage performance, systematic characterizations are performed based on 5p-PEI in comparison to PEI. The DE loops of 5p-PEI and PEI under 200 °C were further investigated to obtain energy storage performance at 200 °C (Figures 2a and S11 and Table S2). With the increase in the electric field, the efficiency decreases owing to the nonlinear increase in the electrical conduction loss. At the working condition of BOPP capacitors, 200 MV/m, the discharged efficiency of PEI is 91%, while the efficiency of 5p-PEI is 95%. Even at 400 MV/m, double the working condition of BOPP, the discharged efficiency for 5p-PEI is still as high as 91%. The discharge efficiencies of the reported polymers or polymer composites at 200 °C are also summarized in Figure 2a.^{9–12,16–18} The maximum electric fields under the DE loops measurement of 5p-PEI and PEI as a function of the temperature are shown in Figure S12. The maximum electric field of 5p-PEI is statistically much higher than that of PEI. At 200 MV/m and 200 °C (the working condition of BOPP), 5p-PEI exhibits stable energy density and high efficiency of >91% during 100 000 cycles of charging and discharging (Figure 2b).

To better understand the energy storage mechanisms, the dielectric constant and loss (dissipation factor) are presented in Figure 3. With changes in frequency and temperature, the dielectric constant is stable for both 5p-PEI and PEI. With the increase in temperature from 40 to 150 °C, the dissipation factor of 5p-PEI is nearly unchanged, while it is increased slightly for PEI at lower frequencies. At 200 °C when the frequency is <10 Hz, although the segmental relaxation of polymer chains leads to higher polarization loss (dissipation factor),¹⁹ the dissipation factor for 5p-PEI still remains lower than that of PEI. The better flexibility of *p*-phenylenediamine relative to *m*-phenylenediamine imparts 5p-PEI with lower dissipation factors probably due to the less energy dissipated in the interactions of adjacent structures in the relaxation processes.²⁰

The high field conduction arising from temperature- and field-dependent charge injection and transport is the major source of energy loss at elevated temperatures and high electric fields.^{2,14,21,22} As the reported quasi-steady-state approach can just deliver conduction current at lower electric fields,²³ we designed a system to measure the electrical conduction under a transient condition.²⁴ The integrated conduction current at

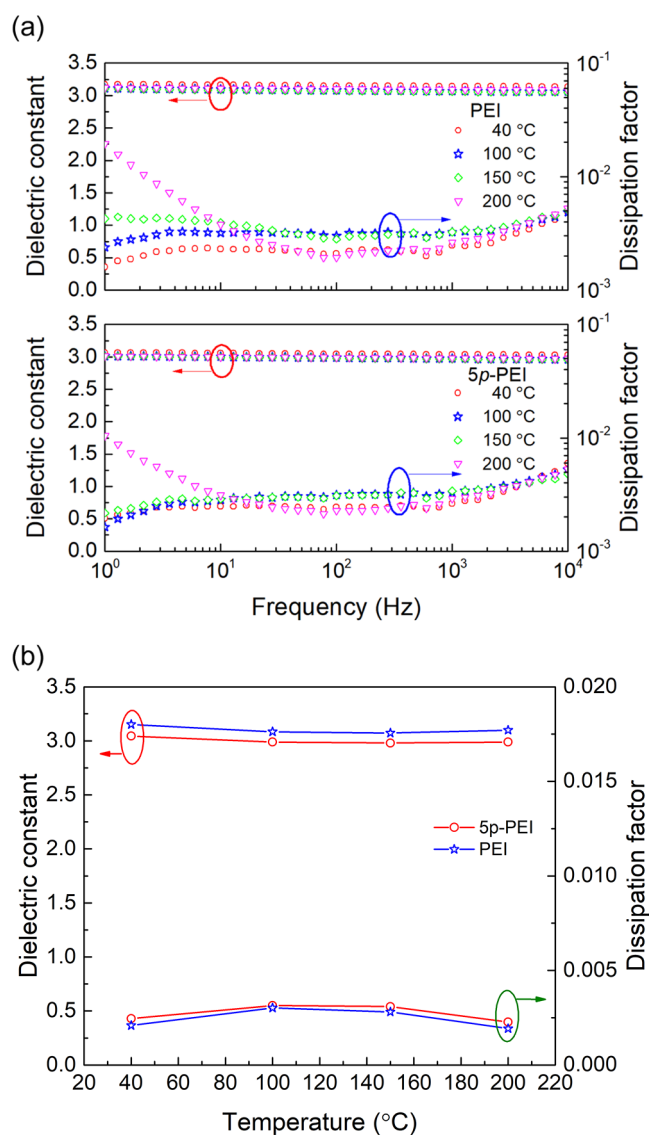


Figure 3. Dielectric polarization. (a) Dielectric constant and dissipation factor of PEI and 5p-PEI as functions of frequency. (b) Temperature dependence of the dielectric constant and dissipation factor at 100 Hz.

150 °C for PEI and 5*p*-PEI is presented in Figure 4. To provide further insights into the conduction mechanism, the

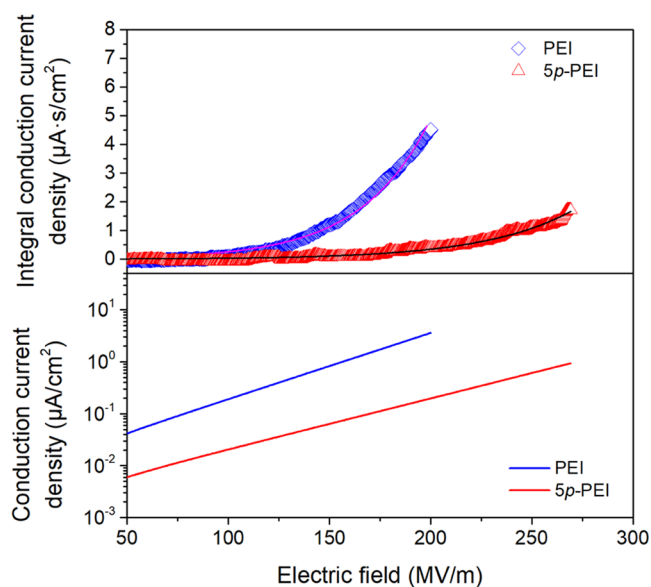


Figure 4. High electric field conduction of PEI and 5*p*-PEI at 150 °C.

hopping conduction model is utilized to calculate the conduction current, as shown in eq 1

$$J = J_0 \frac{\exp\left(\frac{eE\lambda}{2kT}\right) - \exp\left(-\frac{eE\lambda}{2kT}\right)}{2} \quad (1)$$

where T is the temperature (Kelvin), J_0 is proportional to the charge carrier density, e is the charge amount of the carrier, and k is the Boltzmann constant. λ is the hopping distance and E is the electric field. Then, the integral conduction current (ICC) is expressed as

$$\text{ICC} = \int J dt \quad (2)$$

According to eqs 1 and 2, the experimentally investigated integral conduction current can be fitted by the integral form of the hopping conduction, as shown by the solid line. The fitting results compare favorably with the experimental results of the integrated electrical conduction current. According to the fitting, the conduction current is also calculated and shown in Figure 4. The conduction current is more than 1 order of magnitude lower for 5*p*-PEI from a side-by-side comparison with PEI. In the hopping process, the hopping distance between adjacent trapping sites for PEI is 2.1 nm, which is reduced to 1.6 nm for 5*p*-PEI. The kinetic energy of charge carriers accumulated between adjacent trapping sites is λeE . The shorter hopping distance of 5*p*-PEI impeded charge carriers from accumulating more kinetic energy, thus suppressing the conduction, especially at high electric fields. To better understand the underlying mechanism, band gaps are experimentally investigated and computed. Band gap can be considered the major factor and the local state the secondary one that determines the breakdown strength of polymer dielectrics. Polymers with an intrinsically large band gap are more likely to have higher breakdown strength and lower conduction loss.^{2,21,22} Figure S14 shows the experimental band gap plot for control PEI and PEI with structural defects, where insignificant changes could be found for

different polymer structures. It is reasonable because the change in the polymer structure is a local modification. Although the band gap values for original PEI and PEI with different *p*-phenylenediamine amounts are similar (Table S3 Supporting Information), the density functional theory (DFT) computation indicates different densities of states (DOSs) for PEI and modified PEI (Figure S13). The topological disorder of polymer chains through weak van der Waals force leads to localized states.²⁵ The structural modification is likely to strengthen the polymer chain interactions and thus modify the localized states of band structures, leading to the lowered hopping distance. Conjugated aromatic benzene rings are generally introduced to enhance the thermal stability of polymers. The locally improved flexibility of 5*p*-PEI can decouple the pi–pi stacking and conjugation of the aromatic groups, leading to suppressed charge transport.²

In summary, we introduce a small amount of structural modification to PEI to improve the local rotation flexibility of chains. The dissipation factor of 5*p*-PEI with 5% structural modification is <1% owing to the improved flexibility. More importantly, the electrical conduction loss at high electric fields is suppressed by the incorporation of the structural modification, attributed to the modified local defect states, and thus lowered hopping distance. As a result, the new PEI exhibits much higher efficiency, outperforming the best-reported polymers and polymer composites at elevated temperatures up to 200 °C. The strategy of incorporating a tiny amount of structural modification through facile synthesis and processing uncovers an effective way to modify polymer dielectrics for harsh high-field-energy storage.

EXPERIMENTAL SECTION

Material Characterizations. ¹H NMR was performed through a Bruker AVANCE 500 MHz spectrometer. The TMS was used as an internal standard for the measurement. The glass transition temperature was measured using DSC Q-100. Thermogravimetric analysis (TGA) Q-500 was used for the thermogravimetric analysis. The molecular weight was measured using a Waters GPC system. The poly(methyl methacrylate) (PMMA) was used as a standard and dimethylacetamide as the mobile phase. A KBr pellet method with a Nicolet Magna 560 infrared (IR) spectrometer was used for the Fourier transform infrared spectroscopy (FTIR) measurement. The UV–vis spectrum was measured using Varian Cary UV–vis 5000 to obtain the band gap. Polyetherimide films with a thickness of ~10 μm were prepared by the solution cast.

Molecular Dynamics Simulations. Rotational barriers are calculated for *m*-phenylenediamine- and *p*-phenylenediamine-incorporated PEI structures using molecular dynamics simulations. The rotation barrier for these systems is computed by first varying the orientation of chains attached to the phenyl rings followed by a rotation of the ring itself keeping the chains fixed. Various configurations thus obtained are relaxed using a conjugate gradient minimization scheme using a Reax force field. The energies thus obtained for various configurations show that the chain rotation for *p*-phenylenediamine is the lowest, while *m*-phenylenediamine has the highest barrier to chain rotation due to the presence of a doubly conjugated ring in the PEI backbone. Moreover, similar behavior can be seen for the rotation barrier computed for the phenyl rings. These results show that PEI with the structure modification can reorient itself and thus distribute external stress when subjected to external stress.

DFT Computation. All DFT computations were performed using VASP with a Perdew–Burke–Ernzerhof exchange–correlation functional and a plane-wave energy cutoff of 400 eV. In the calculations, PEI models were constructed by oligomers with two repeat units (connected by defects) and optimized using the Monkhorst–Pack k -

point meshes of $1 \times 1 \times 1$. The electronic structure of PEI with and without defects was estimated using HSE06 functional. The physical and electronic structures of PEI are shown in Figure S6a,b.

Electrical Characterization. A Solartron SI 1260 frequency response analyzer in combination with a Solartron 1296 dielectric interface was used to measure the dielectric constant and dissipation factor. DE loop was measured using a modified Sawyer–Tower tester under a voltage of 100 Hz using a positive unipolar sinusoidal waveform. Gold/palladium electrodes with a 3 mm diameter were deposited on the surface of polymer films using the sputter coating method.

■ ASSOCIATED CONTENT

SI Supporting Information

The Supporting Information is available free of charge at <https://pubs.acs.org/doi/10.1021/acs.chemmater.2c01441>.

Synthesis scheme of polymer; NMR spectra; thermogravimetric analysis curves; differential scanning calorimetry scans; energy density and discharged efficiency curves; D – E loop plots, and UV band gap plots (PDF)

■ AUTHOR INFORMATION

Corresponding Authors

Yang Cao – Electrical Insulation Research Center, Institute of Materials Science, University of Connecticut, Storrs, Connecticut 06269, United States; Department of Electrical and Computer Engineering, University of Connecticut, Storrs, Connecticut 06269, United States; orcid.org/0000-0001-7034-2792; Email: yang.cao@uconn.edu

Gregory Sotzing – Institute of Materials Science, University of Connecticut, Storrs, Connecticut 06269, United States; Department of Chemistry, University of Connecticut, Storrs, Connecticut 06269, United States; Email: g.sotzing@uconn.edu

Authors

Abdullah Alamri – Institute of Materials Science, University of Connecticut, Storrs, Connecticut 06269, United States; orcid.org/0000-0002-6857-265X

Chao Wu – Electrical Insulation Research Center, Institute of Materials Science, University of Connecticut, Storrs, Connecticut 06269, United States; orcid.org/0000-0002-4565-8231

Ankit Mishra – Collaboratory for Advanced Computing and Simulations, Department of Chemical Engineering and Materials Science, Department of Physics & Astronomy, and Department of Computer Science, University of Southern California, Los Angeles, California 90089, United States

Lihua Chen – School of Materials Science and Engineering, Georgia Institute of Technology, Atlanta, Georgia 30332, United States; orcid.org/0000-0002-9852-8211

Zongze Li – Electrical Insulation Research Center, Institute of Materials Science, University of Connecticut, Storrs, Connecticut 06269, United States; Department of Electrical and Computer Engineering, University of Connecticut, Storrs, Connecticut 06269, United States

Ajinkya Deshmukh – Institute of Materials Science, University of Connecticut, Storrs, Connecticut 06269, United States

Jierui Zhou – Electrical Insulation Research Center, Institute of Materials Science, University of Connecticut, Storrs, Connecticut 06269, United States; Department of Electrical and Computer Engineering, University of Connecticut, Storrs, Connecticut 06269, United States

Omer Yassin – Department of Chemistry, University of Connecticut, Storrs, Connecticut 06269, United States

Rampi Ramprasad – School of Materials Science and Engineering, Georgia Institute of Technology, Atlanta, Georgia 30332, United States; orcid.org/0000-0003-4630-1565

Priya Vashishta – Collaboratory for Advanced Computing and Simulations, Department of Chemical Engineering and Materials Science, Department of Physics & Astronomy, and Department of Computer Science, University of Southern California, Los Angeles, California 90089, United States; orcid.org/0000-0003-4683-429X

Complete contact information is available at:

<https://pubs.acs.org/10.1021/acs.chemmater.2c01441>

Author Contributions

[▽]A.A. and C.W. contributed equally to this work.

Author Contributions

G.A.S. conceived the idea of defects for lowering the rotational energy barrier and both G.A.S. and Y.C. directed the research. A.A. and C.W. contributed equally to the experiments and manuscript preparation. A.A. and A.D. synthesized the monomers and polymers and conducted characterization experiments. C.W., Z.L., and J.Z. performed electrical experiments. A.M. and P.V. computed rotation energy barrier. L.C. and R.R. conducted the electronic structure simulations. A.A. and C.W. wrote the first manuscript and all authors participated in editing the manuscript.

Notes

The authors declare no competing financial interest.

■ ACKNOWLEDGMENTS

The authors would like to acknowledge the financial support from a capacitor program grant (N0014-19-1-2340) and a multidisciplinary university research initiative (MURI) grant (N00014-17-1-2656), both from ONR.

■ REFERENCES

- (1) Pan, H.; Li, F.; Liu, Y.; Zhang, Q.; Wang, M.; Lan, S.; Zheng, Y.; Ma, J.; Gu, L.; Shen, Y.; Yu, P.; Zhang, S.; Chen, L.-Q.; Lin, Y.-H.; Nan, C.-W. Ultrahigh-Energy Density Lead-Free Dielectric Films via Polymorphic Nanodomain Design. *Science* **2019**, *365*, 578–582.
- (2) Wu, C.; Deshmukh, A. A.; Li, Z.; Chen, L.; Alamri, A.; Wang, Y.; Ramprasad, R.; Sotzing, G. A.; Cao, Y. Flexible Temperature-Invariant Polymer Dielectrics with Large Bandgap. *Adv. Mater.* **2020**, *32*, No. 2000499.
- (3) Mannodi-Kanakkithodi, A.; Treich, G. M.; Huan, T. D.; Ma, R.; Tefferi, M.; Cao, Y.; Sotzing, G. A.; Ramprasad, R. Rational Co-Design of Polymer Dielectrics for Energy Storage. *Adv. Mater.* **2016**, *28*, 6277–6291.
- (4) Sharma, V.; Wang, C.; Lorenzini, R. G.; Ma, R.; Zhu, Q.; Sinkovits, D. W.; Pilania, G.; Oganov, A. R.; Kumar, S.; Sotzing, G. A.; Boggs, S. A.; Ramprasad, R. Rational Design of All Organic Polymer Dielectrics. *Nat. Commun.* **2014**, *5*, No. 4845.
- (5) Zhang, T.; Chen, X.; Thakur, Y.; Lu, B.; Zhang, Q.; Runt, J.; Zhang, Q. M. A Highly Scalable Dielectric Metamaterial with Superior Capacitor Performance over a Broad Temperature. *Sci. Adv.* **2020**, *6*, No. eaax6622.
- (6) Ho, J. S.; Greenbaum, S. G. Polymer Capacitor Dielectrics for High Temperature Applications. *ACS Appl. Mater. Interfaces* **2018**, *10*, 29189–29218.
- (7) Buttay, C.; Planson, D.; Allard, B.; Bergogne, D.; Bevilacqua, P.; Joubert, C.; Lazar, M.; Martin, C.; Morel, H.; Tournier, D.; Raynaud,

C. State of the Art of High Temperature Power Electronics. *Mater. Sci. Eng.: B* **2011**, *176*, 283–288.

(8) Tan, D.; Zhang, L.; Chen, Q.; Irwin, P. High-Temperature Capacitor Polymer Films. *J. Electron. Mater.* **2014**, *43*, 4569–4575.

(9) Azizi, A.; Gadinski, M. R.; Li, Q.; AlSaud, M. A.; Wang, J.; Wang, Y.; Wang, B.; Liu, F.; Chen, L. Q.; Alem, N.; Wang, Q. High-Performance Polymers Sandwiched with Chemical Vapor Deposited Hexagonal Boron Nitrides as Scalable High-Temperature Dielectric Materials. *Adv. Mater.* **2017**, *29*, No. 1701864.

(10) Li, Q.; Chen, L.; Gadinski, M. R.; Zhang, S.; Zhang, G.; Li, H. U.; Iagodkine, E.; Haque, A.; Chen, L.-Q.; Jackson, T. N.; Wang, Q. Flexible High-Temperature Dielectric Materials from Polymer Nanocomposites. *Nature* **2015**, *523*, 576–579.

(11) Li, H.; Ai, D.; Ren, L.; Yao, B.; Han, Z.; Shen, Z.; Wang, J.; Chen, L.; Wang, Q. Scalable Polymer Nanocomposites with Record High-Temperature Capacitive Performance Enabled by Rationally Designed Nanostructured Inorganic Fillers. *Adv. Mater.* **2019**, *31*, No. 1900875.

(12) Yuan, C.; Zhou, Y.; Zhu, Y.; Liang, J.; Wang, S.; Peng, S.; Li, Y.; Cheng, S.; Yang, M.; Hu, J.; Zhang, B.; Zeng, R.; He, J.; Li, Q. Polymer/Molecular Semiconductor All-Organic Composites for High-Temperature Dielectric Energy Storage. *Nat. Commun.* **2020**, *11*, No. 3919.

(13) Li, H.; Gadinski, M. R.; Huang, Y.; Ren, L.; Zhou, Y.; Ai, D.; Han, Z.; Yao, B.; Wang, Q. Crosslinked Fluoropolymers Exhibiting Superior High-Temperature Energy Density and Charge–Discharge Efficiency. *Energy Environ. Sci.* **2020**, *13*, 1279–1286.

(14) Zhang, B.; Liu, J.; Ren, M.; Wu, C.; Moran, T. J.; Zeng, S.; Chavez, S. E.; Hou, Z.; Li, Z.; LaChance, A. M.; Jow, T. R.; Huey, B. D.; Cao, Y.; Sun, L. Reviving the “Schottky” Barrier for Flexible Polymer Dielectrics with a Superior 2D Nanoassembly Coating. *Adv. Mater.* **2021**, *33*, No. 2101374.

(15) Wu, C.; Alamri, A.; Deshmukh, A. A.; Li, Z.; Islam, S.; Sotzing, G. A.; Cao, Y. In *A Modified Polyetherimide Film Exhibiting Greatly Suppressed Conduction for High-Temperature Dielectric Energy Storage*, IEEE Conference on Electrical Insulation and Dielectric Phenomena (CEIDP), 2020; pp 451–454.

(16) Xu, D.; Xu, W.; Seery, T.; Zhang, H.; Zhou, C.; Pang, J.; Zhang, Y.; Jiang, Z. Rational Design of Soluble Polyaramid for High-Efficiency Energy Storage Dielectric Materials at Elevated Temperatures. *Macromol. Mater. Eng.* **2020**, *305*, No. 1900820.

(17) Zhang, Q.; Chen, X.; Zhang, B.; Zhang, T.; Lu, W.; Chen, Z.; Liu, Z.; Kim, S. H.; Donovan, B.; Warzoha, R. J.; Gomez, E. D.; Bernholc, J.; Zhang, Q. M. High-Temperature Polymers with Record-High Breakdown Strength Enabled by Rationally Designed Chain-Packing Behavior in Blends. *Matter* **2021**, *4*, 2448–2459.

(18) Dong, J.; Hu, R.; Xu, X.; Chen, J.; Niu, Y.; Wang, F.; Hao, J.; Wu, K.; Wang, Q.; Wang, H. A Facile In Situ Surface-Functionalization Approach to Scalable Laminated High-Temperature Polymer Dielectrics with Ultrahigh Capacitive Performance. *Adv. Funct. Mater.* **2021**, *31*, No. 2102644.

(19) Kremer, F.; Schönhals, A. *Broadband Dielectric Spectroscopy*; Springer Berlin Heidelberg: Berlin, Heidelberg, 2003.

(20) Wu, C.; Li, Z.; Treich, G. M.; Tefferi, M.; Casalini, R.; Ramprasad, R.; Sotzing, G. A.; Cao, Y. Dipole-Relaxation Dynamics in a Modified Polythiourea with High Dielectric Constant for Energy Storage Applications. *Appl. Phys. Lett.* **2019**, *115*, No. 163901.

(21) Ieda, M. Electrical Conduction and Carrier Traps in Polymeric Materials. *IEEE Trans. Electr. Insul.* **1984**, *EI-19*, 162–178.

(22) Dissado, L. A.; Fothergill, J. C. *Electrical Degradation and Breakdown in Polymers*; Institution of Engineering and Technology, 1992.

(23) Xu, C.; Boggs, S. In *Measurement of Resistive and Absorption Currents in Capacitor Films up to Breakdown*, Conference Record of the 2006 IEEE International Symposium on Electrical Insulation, 2006; pp 249–252.

(24) Li, Z.; Xu, C.; Uehara, H.; Boggs, S.; Cao, Y. Transient Characterization of Extreme Field Conduction in Dielectrics. *AIP Adv.* **2016**, *6*, No. 115025.

(25) Ishii, H.; Sugiyama, K.; Ito, E.; Seki, K. Energy Level Alignment and Interfacial Electronic Structures at Organic/Metal and Organic/Organic Interfaces. *Adv. Mater.* **1999**, *11*, 605–625.

Recommended by ACS

Constructing High-Performance Dielectrics via Molecular and Phase Engineering in Dipolar Polymers

Haoran Xu, Dou Zhang, *et al.*

FEBRUARY 12, 2021
ACS APPLIED ENERGY MATERIALS

READ 

All-Organic Polymer Dielectrics Containing Sulfonyl Dipolar Groups and π - π Stacking Interaction in Side-Chain Architectures

Haoran Xu, Dou Zhang, *et al.*

AUGUST 31, 2021
MACROMOLECULES

READ 

Chemically Controlled Volatile and Nonvolatile Resistive Memory Characteristics of Novel Oxygen-Based Polymers

Brian J. Ree, Toshifumi Satoh, *et al.*

JUNE 11, 2020
ACS APPLIED MATERIALS & INTERFACES

READ 

Thermal Conductivity of Pentiptycene-Based Poly(*o*-hydroxyimide) Copolymers: A Study via Integrated Experiments and Simulations

Xingfei Wei, Tengfei Luo, *et al.*

MAY 18, 2021
ACS APPLIED POLYMER MATERIALS

READ 

Get More Suggestions >